AJNR Am J Neuroradiol 24:444–450, March 2003

Cortical Blood Flow during Cerebral Vasospasm after Aneurysmal Subarachnoid Hemorrhage: Three-Dimensional *N*-Isopropyl-*p*-[^{123}I]Iodoamphetamine Single Photon Emission CT Findings

Hiroki Ohkuma, Shigeharu Suzuki, Kanae Kudo, Shafiqul Islam, and Tomonari Kikkawa

BACKGROUND AND PURPOSE: **The relationship between regional cerebral blood flow (rCBF) during cerebral vasospasm after subarachnoid hemorrhage (SAH) and angiographic vasospasm and the value of rCBF in predicting vasospasm and the prognosis are not fully delineated. Our aim was to investigate the changes in extent of vasospasm-induced decreased cortical rCBF on three-dimensional (3D) displays of single photon emission CT (SPECT) findings. The clinical usefulness of these assessments was analyzed.**

METHODS: **In 58 cases of SAH, SPECT and digital subtraction angiography were performed on the same day, 5–9 days after SAH or within 24 hours after the onset of delayed ischemic neurologic deficit (DIND). Cerebral blood flow data were assessed by measuring the area of decreased cortical rCBF on 3D SPECT images.**

RESULTS: **The area of decreased cortical rCBF on the 3D images was significantly increased in cases with DIND ($P < .001$), in cases with a large infarction due to vasospasm ($P = .006$), and in cases with a poor prognosis after vasospasm ($P = .045$). These increases were also related to the type of angiographic vasospasm; the greatest decrease in cortical rCBF occurred in the combined type (combination of the peripheral and proximal types) of vasospasm, followed by cases with the peripheral type, proximal type, and no angiographic vasospasm. In cases with DIND, patchy decreased cortical rCBF areas were seen before the onset of DIND.**

CONCLUSION: **Combined-type vasospasm leads to reductions in CBF greater than those due to isolated peripheral or proximal vasospasm. Two-dimensional and mean-hemispheric CBF analyses are less sensitive for this change than is 3D SPECT.**

Cerebral vasospasm associated with aneurysmal subarachnoid hemorrhage (SAH) is angiographically characterized by a persistent luminal narrowing of the major extraparenchymal cerebral arteries. This affects a patient's prognosis by causing decreased cerebral blood flow (CBF) and delayed ischemic neurologic deficit (DIND). Many studies have been performed to investigate the changes of CBF during cerebral vasospasm (1–19); however, the results of these studies are equivocal, and the relationship between the changes of CBF and the degree of angiographic vasospasm, the degree of DIND, and a patient's prognosis have yet to be fully understood. In addition, its value in predicting the occurrence of cerebral vasospasm is unclear.

Changes in CBF during cerebral vasospasm can be evaluated as the degree of CBF decrease at the region of interest (ROI) (1, 2, 4, 7–9, 18, 19) or mean CBF in a global region such as the cerebral hemisphere (3, 5–11, 14–17). Because cerebral vasospasm mainly affects the regional CBF (rCBF) in the cerebral cortex (13, 19), an evaluation of the extent of the decreased cortical rCBF would be useful for clarifying the pathogenesis of cerebral vasospasm and predicting patients' clinical course and prognosis. Recently, three-dimensional (3D) displays of cerebral cortical CBF on single photon emission CT (SPECT) images have become available for routine clinical use (20, 21). Thus, the routine evaluation of the extent of decreased cortical rCBF has become more feasible,

Received May 28, 2002; accepted after revision September 2.

From the Department of Neurosurgery, Hirosaki University School of Medicine, Japan.

Address reprint requests to Hiroki Ohkuma, MD, Department of Neurosurgery, Hirosaki University School of Medicine, 5 Zaifucho, Hirosaki, 036-8216 Japan.

offering ease of use and a precise measurement capability. The aim of this study was to investigate the changes in the extent of decreased cortical rCBF on 3D SPECT images and to correlate these changes with both the degree of angiographic vasospasm and the patient's clinical course. We thus hoped to determine if rCBF assessment is useful in assessing a patient's clinical condition and in predicting prognosis.

Methods

Subjects

This study was prospectively performed from April 1995 to March 1999. During this period, 112 cases of aneurysmal SAH in 112 patients and in which the diagnosis was confirmed with CT and cerebral angiography were treated at our institute. Of the 112 patients, 58 patients who underwent aneurysm surgery within 48 hours after the onset of SAH were younger 70 years. They had SAH findings corresponding to group 2 or 3, according to the Fisher classification on the initial CT scan. These patients were included in this study. These 58 patients routinely underwent SPECT with *N*-isopropyl-*p*-[^{123}I]iodoamphetamine (^{123}I-IMP) and digital subtraction angiography (DSA) on the same day, 5–9 days after SAH, to prophylactically induce hypertension on the basis of the angiographic findings before DIND occurred. Prophylactically induced hypertension was achieved by maintaining a mean arterial blood pressure of between 105 and 120 mm Hg. In addition to these routine examinations, if DIND occurred, ^{123}I-IMP SPECT followed by DSA was again performed within 24 hours after the onset of DIND. The patients were considered to have DIND due to vasospasm when a focal neurologic deficit or deterioration in level of consciousness was documented and when other possible causes of deterioration, such as rebleeding, hydrocephalus, surgical complication, electrolyte disorder, andinfection or seizure, were excluded. The CBF data derived from ^{123}I-IMP SPECT were stratified according to the presence or absence of DIND, angiographic vasospasm, the size of the infarction on the CT scans, and the patient's prognosis.

^{123}I-IMP SPECT Analysis

The rCBF was estimated by using the ^{123}I-IMP autoradiographic (ARG) method (5, 22). We used a rotating-type gamma camera, Starcam 4000XR/T (GE Medical Systems, Milwaukee, WI) with a low-energy and high-resolution collimator with a full width at half maximum of 8.1 mm. Thirty minutes after the intravenous injection of 222 MBq ^{123}I-IMP, data acquisition was started for a scanning duration of 20 minutes so that the midscan time was 40 minutes. At 10 minutes after the administration of IMP, 3 mL of arterial blood was obtained from the brachial artery, and the whole-blood radioactivity was measured by using a well counter that was cross-calibrated with SPECT. The assumed distribution volume of IMP (*Vd*) for the ARG method was determined by comparing the rCBF obtained by the table look-up method with the value obtained by using the ARG method (24). A good correlation between the values was achieved when *Vd* was 55 ($Y = 1.145X - 2.823$, $r = 0.990$) ($P < .001$, Pearson correlation coefficient). Surface and volume 3D images were reconstructed from the transaxial SPECT data (Fig 1A). The surface threshold value was set at 30 mL/100 g/min, and the region with rCBF less than 30 mL/100 g/min was displayed as an image defect (Fig 1B).

The CBF data were assessed by using the following three methods: 1) determining the rCBF in the ROI on two-dimensional (2D) images; 2) calculating the mean hemispheric CBF by using 2D images; 3) and analyzing the area of decreased cortical rCBF on 3D images. Using the first method, the rCBF in the ROI, the decreased rCBF portion of the cortical region was selected by mean of visual inspection of the 2D images. An rCBF at ROI consisting of a 15 × 30-mm area of the cerebral cortex was set in the center of the decreased rCBF portion on the 2D image, and the rCBF value was measured (Fig 1C). Using the second method, the mean hemispheric CBF was calculated with all of the transaxial data for the 2D images. In cases with a middle cerebral artery (MCA) aneurysm and in those with an internal carotid artery (ICA) aneurysm, the hemisphere with the aneurysm was used for the evaluation of the mean hemispheric CBF. In cases with an anterior communicating (ACoA) aneurysm and in those with an anterior cerebral artery and anterior cerebral artery (ACA) aneurysm, the hemisphere with less CBF data was used for the evaluation of

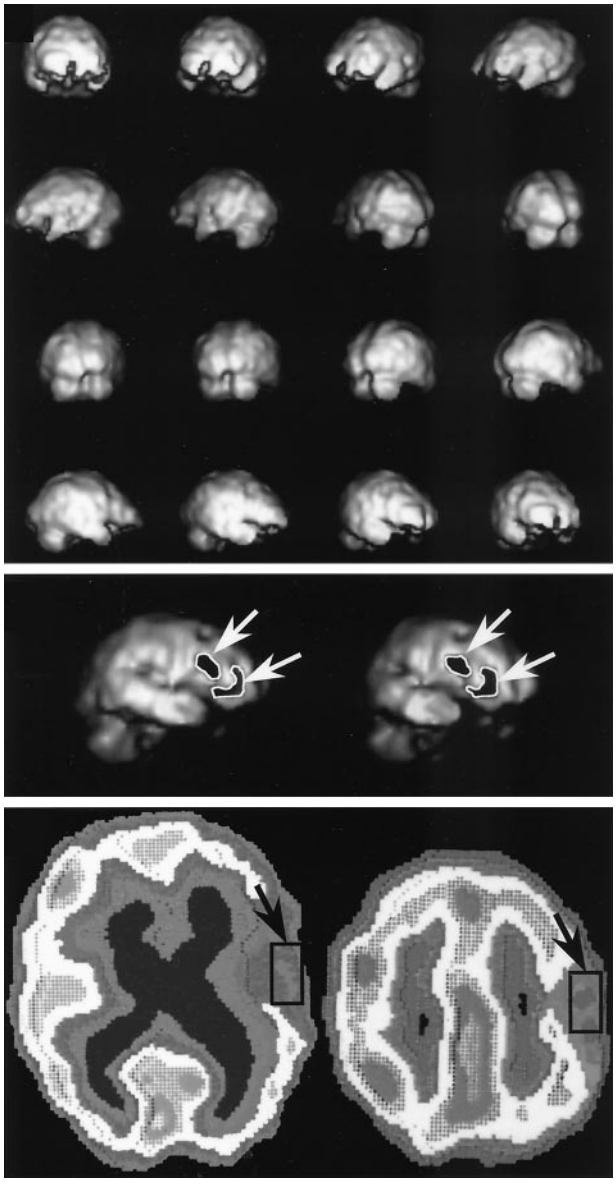

FIG 1. Methods of rCBF assessment.

Top, 3D images were made by reconstructing the transaxial SPECT data.

Middle, The surface threshold value was set at 30 mL/100 g/min, and the image defects, which indicate the region with rCBF less than 30 mL/100 g/min, were outlined and calculated by using the image-analysis system (*arrows*).

Bottom, Transaxial images were obtained with the IMP-ARG method. ROIs of 30 × 15 mm were set in the lesion with decreased CBF along the cerebral cortex (*arrows*), and its value was measured.

the mean hemispheric CBF. Using the third method, the region with a cortical rCBF of less than 30 mL/100 g/min was displayed as an image defect on the 3D images. The images were stored in the computer system. The region of decreased cortical rCBF less than 30 mL/100 g/min was outlined, and its area was calculated by using the image-analysis system (Fig 1B). To test the interobserver variability in the measurement of the rCBF data with the first and third methods, two observers (M.S.I., T.K.) who did not have knowledge of the other results independently determined the measures in the same manner just described. A strong correlation between the two measures were obtained for the first method ($r = 0.918$, $P < .001$) and for the third method ($r = 0.945$, $P < .001$) with the Spearman rank correlation coefficient.

Evaluation of Angiographic Vasospasm

The degree of angiographic vasospasm was evaluated on DSA images by comparing the caliber of the lumen on preoperative angiograms with the caliber on postoperative routine angiograms or on angiograms obtained in the event of the onset of DIND. Cerebral angiography was performed by injecting the contrast agent into the ICA through a 5F selective catheter inserted via the femoral artery into each ICA. DSA images were obtained by using a DSA unit (Advantx; GE Medical Systems) with a pixel matrix of 512 × 512. Theses were stored on a computer system (Macintosh; Apple Computer, Cupertino, CA). The evaluation of vasospasm was performed not only in the proximal main arteries but also in the peripheral portion of those arteries. The evaluation of the proximal type of angiographic vasospasm was performed by measuring the caliber of the lumen caliber in the horizontal portion of the middle cerebral artery (M1), in the horizontal portion of the anterior cerebral artery (A1), and in intradural portion of the ICA. Each arterial portion was divided into three equal-length portions, the diameters at the midpoint of each of these divided portions were measured, and the mean values were calculated. The peripheral type of angiographic vasospasm was evaluated by measuring the caliber of the lumen in the insular portions of the middle cerebral arteries (M2) or in the peripheral portions of the anterior cerebral artery (A2). The midpoint of each arterial portion was measured, and the mean values were calculated. To test the interobserver variability in the measurement of arterial diameter, two observers (M.S.I., T.K.) who did not have knowledge of the other results independently measured the arterial diameters in the same manner as that just described. This analysis revealed a strong correlation between the two measures ($r = 0.982$, $P < .001$, Spearman rank correlation coefficient). Angiographic vasospasm at each portion was judged to have occurred when arterial diameter reduction exceeded 50%. On the basis of these evaluations, angiographic vasospasm was categorized into four groups: 1) no angiographic vasospasm when angiographic vasospasm had not occurred in the peripheral or proximal; 2) proximal type of angiographic vasospasm when angiographic vasospasm had occurred in only the proximal portion; 3) peripheral type of angiographic vasospasm when angiographic vasospasm had occurred in only the peripheral portion; and 4) combined type of angiographic vasospasm when angiographic vasospasm had occurred in both the proximal portion and the peripheral portion.

Infarction Size on CT Scans

The size of infarction was evaluated by measuring the longest diameter of the hypoattenuated area on CT scans obtained at least 3 weeks after the onset of DIND. These lesions were categorized as large when the diameter was more than 4 cm and as small when the diameter was less than 4 cm.

Prognosis at 3 Months

The patient's prognosis was evaluated at 3 months after SAH by using the Glasgow Outcome Coma Scale. Good recovery and moderate disability on the scale were categorized as a fair prognosis. Severe disability, a vegetative state, and death were categorized as a poor prognosis.

Statistical Analysis

Clinical parameters such as age, sex, site of aneurysm, Hunt and Hess grade on admission, and SAH on the initial CT scan were compared between the cases with DIND and those without DIND. For this comparison, the $\div^2$ test, Mann-Whitney *U* test, or Student *t* test was used. The CBF data for each group were compared by using the Mann-Whitney *U* test. Statistical significance was assigned at $P < .05$.

Results

Of 58 cases, 15 cases involved DIND due to cerebral vasospasm 5–14 days after the onset of SAH, whereas the other 43 cases did not involve DIND. The clinical parameters of these 15 cases with DIND were compared with those of the 43 cases without DIND (Table 1), and no statistically significant differences were seen between the two groups.

DIND and rCBF

The rCBF data obtained at the onset of DIND in the 15 cases with DIND were compared with the data obtained 5–9 days after SAH during routine studies in the 43 cases without DIND (Table 2). The rCBF in the ROI on conventional 2D displays was significantly lower in the cases with DIND ($P < .001$) than in the others. However, the mean hemispheric CBF was not significantly different between the two groups. The area of decreased cortical rCBF, as measured on 3D displays, was significantly increased in the DIND cases ($P < .001$). 3D images of cortical rCBF in the cases with DIND are shown in Figure 2.

TABLE 1: Clinical parameters in cases with DIND and cases without DIND

Parameter	Cases without DIND (n = 43)	Cases with DIND (n = 15)
Mean age ± SD, y	56.8 ± 10.5	54.2 ± 11.6
Sex ratio (male/female)	14/29	4/11
Site of aneurysms*		
ICA	14 (33)	6 (40)
MCA	13 (30)	5 (33)
ACA and ACoA	16 (37)	4 (27)
Hunt and Hess grade*		
1 and 2	22 (51)	7 (47)
3	18 (35)	5 (33)
4 and 5	3 (7)	3 (20)
Fisher classification of SAH on CT scans*		
Group 2	11 (26)	2 (13)
Group 3	32 (74)	13 (87)

* Data in parentheses are percentages.

TABLE 2: CBF data

Measure	rCBF in ROI on 2D Displays, mL/100g/min	Mean Hemispheric CBF on 2D Displays, mL/100g/min	Area of Decreased Cortical CBF on 3D Displays, cm^2
Cases*			
With DIND (n = 15)	25.0 ± 5.1†	35.5 ± 5.5	22.6 ± 10.0†
Without DIND (n = 43)	37.0 ± 4.8	38.0 ± 5.3	7.4 ± 6.6
Size of infarction‡			
Large (n = 5)	21.8 ± 4.3	32.6 ± 3.8	32.3 ± 6.6§
Small (n = 10)	26.6 ± 4.6	36.9 ± 5.8	17.8 ± 7.5
Prognosis at 3 mo‡			
Poor (n = 6)	22.2 ± 4.2	33.7 ± 4.8	29.8 ± 7.9‖
Fair (n = 9)	26.9 ± 4.5	36.7 ± 5.8	17.8 ± 8.4

* The CBF data obtained at the onset of DIND in the 15 DIND cases were compared with the data on routine studies in the 43 cases without DIND.

† $P < .001$ compared with cases without DIND.

‡ The CBF data obtained at the onset of DIND in the 15 DIND cases were compared.

§ $P = .006$ compared with small size of infarction.

‖ $P = .043$ compared with fair prognosis.

Angiographic Vasospasm, Arterial Diameter, and rCBF

DSA and rCBF data gathered during routine examination in the 43 cases without DIND and at the onset of DIND in the 15 cases with DIND were evaluated according to their arterial diameter at DSA (Fig 3). The rCBF in the ROI on conventional 2D displays was significantly lower in the proximal-type cases, in the peripheral-type cases, and in the combined-type cases of angiographic vasospasm, as compared with the rCBF in cases with no angiographic vasospasm ($P < .001$, $P < .001$, and $P < .001$, respectively). However, no significant differences were seen among the different types of angiographic vasospasm. Mean hemispheric CBF was also significantly lower in the proximal-type cases, in the peripheral-type cases, and in the combined-type cases of angiographic vasospasm, as compared with the cases with no angiographic vasospasm ($P = .027$, $P = .031$, and $P = .002$, respectively). However, no statistically significant differences were seen among the different types of angiographic vasospasm. Evaluation of 3D SPECT images revealed that the size of decreased cortical rCBF was related to the type of angiographic vasospasm. The greatest decrease in cortical rCBF occurred in the combined type of vasospasm, followed in order by the peripheral type, the proximal type, and the cases with no angiographic vasospasm, with statistically significant differences (Fig 3C).

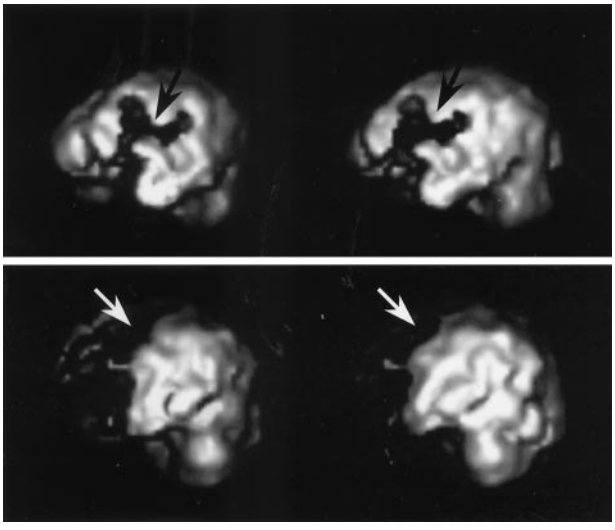

FIG 2. Characteristic findings in cases with DIND.
Top, Image shows widely decreased cortical rCBF at the left MCA region (*arrows*).
Bottom, Image shows widely decreased cortical rCBF at the left ACA region (*arrows*).

Infarction on CT Scans and rCBF

In the 15 cases with DIND, the rCBF data were compared according to infarct size on CT scan (Table 2). The rCBF in the ROI and the mean hemispheric CBF on 2D displays were not significantly different when the cases were categorized into the small- and large-infarction groups. However, the area of decreased cortical rCBF on 3D displays was significantly different between the two groups; the patients in the large-infarction group had the greatest decrease in cortical rCBF ($P = .006$).

Prognosis and rCBF

In the 15 DIND cases, rCBF data were compared according to prognosis at 3 months after SAH (Table 2). The rCBF in the ROI and the mean hemispheric CBF on 2D displays were not significantly different between the cases with a fair prognosis and those with a poor prognosis. However, the area of decreased cortical rCBF on 3D displays did show a statistically significant difference between the two groups; the patients with decreased cortical rCBF had a poorer prognosis ($P = .043$).

rCBF Before the Onset of DIND

In the 15 DIND cases, 10 cases showed symptomatic vasospasm 3–6 days after routine examination, and the patients underwent repeated examinations. The rCBF data gathered on routine examination were compared in these 10 DIND cases and in the 43 cases without DIND. In the cases with DIND, the rCBF in the ROI and the mean hemispheric CBF on 2D dis-

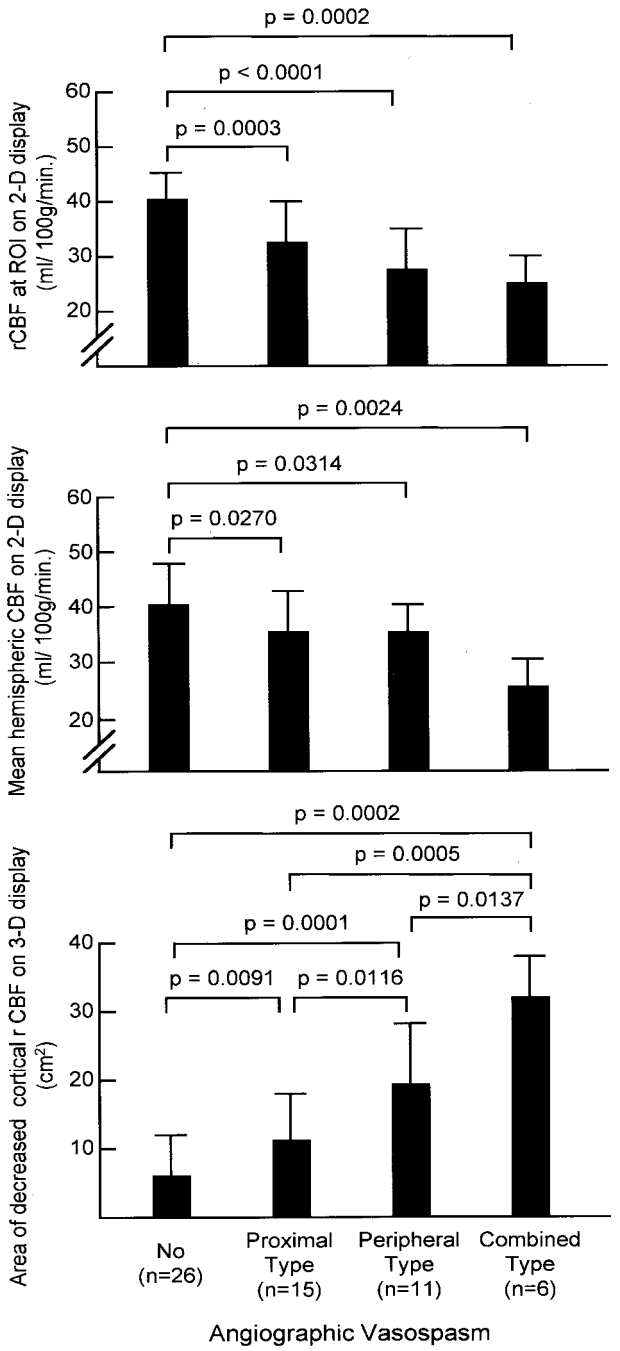

FIG 3. CBF data in all cases compared according to the type of angiographic vasospasm.

Top, rCBF in the ROI on 2D images.

Middle, Mean hemispheric CBF calculated by using 2D images.

Bottom, The area of decreased cortical rCBF measured on 3D images.

play were 34.5 mL/100 g/min ± 4.5 and 37.0 mL/100 g/min ± 4.4, respectively. Values in the cases without DIND were 37.0 mL/100 g/min ± 4.8 and 38.0 mL/100 g/min ± 5.3, respectively. In both evaluations, no statistically significant differences were seen between the cases with DIND and those without DIND. The area of decreased cortical rCBF measured on 3D displays in the cases with DIND and in those without DIND were 15.7 cm^2 ± 6.7 and 9.3 cm^2 ± 8.2, respectively. The difference between the two groups was significantly different; greater decreases in cortical rCBF were seen in the DIND cases ($P = .0219$). In the DIND cases, the multiple, patchy lesions with decreased rCBF were characteristically seen during routine examination performed before the onset of DIND in eight of the 10 cases with DIND (Fig 4).

Discussion

In this study, the effect of cerebral vasospasm on cortical rCBF was evaluated on 2D and 3D displays of ^{123}I-IMP SPECT images. As a quantitative analysis of CBF with IMP SPECT, the IMP-ARG method that we used in this study has recently become well established. This is because of its high reproducibility in patients with stroke and its high sensitivity to cerebral hypoperfusion consistent with that of positron emission tomography (PET) (23, 24). This method is appropriate for routine clinical use, as it requires only one-point arterial blood sampling and a single SPECT scan. These 3D images are easily obtained by reconstructing each horizontal image on a computer. In this study, 30 mL/100 g/min was used as a cut-off point, because in the evaluation of the IMP-ARG method, ischemic symptoms less than 30 mL/100 g/min were seen; infarction can be seen on CT scans when the rCBF is less than 20 mL/100 g/min (5, 19). In this study, the cortical region with flow less than 30 mL/min/100 g was displayed as an image defect on the 3D display. The area of this region can be easily calculated by using the computer.

Many studies involving various methods have been conducted to investigate CBF changes during cerebral vasospasm (1–19). For these evaluations, the following have been used: xenon-133 inhalation and emission CT (1, 3, 11), intraarterial xenon-133 injection and extracranial scintillation detectors (2, 6–8), intravenous technetium-99m injection and a gamma scintillation camera (9, 10), SPECT with technetium-99m-hexamethylpropyleneamine oxime (4, 12, 18), and IMP (19) and PET (14–17). Unfortunately, these studies have yielded equivocal results.

Several studies have shown that focally decreased rCBF is caused by angiographic vasospasm (2–9, 15, 17, 19), especially when severe angiographic vasospasm (luminal reduction of more than 50%) is present (5, 6, 17). However, in moderate angiographic vasospasm, the correlation between the degree of luminal reduction and the degree of rCBF reduction is less clear (11, 19). Controversy exists regarding the correlation of angiographic vasospasm and the global CBF or the mean hemispheric CBF. Some studies have indicated that angiographic vasospasm has no influence on global or mean hemispheric CBF (7, 10). Of course, decreases in rCBF are not solely caused by angiographically documented vasospasm (12, 14, 17). In fact, in these same studies, the angiographic vasospasm was mainly evaluated in the proximal main arteries. Thus, the controversial results concerning the relationship of angiographic vasospasm and rCBF changes are likely the result of factors other than the

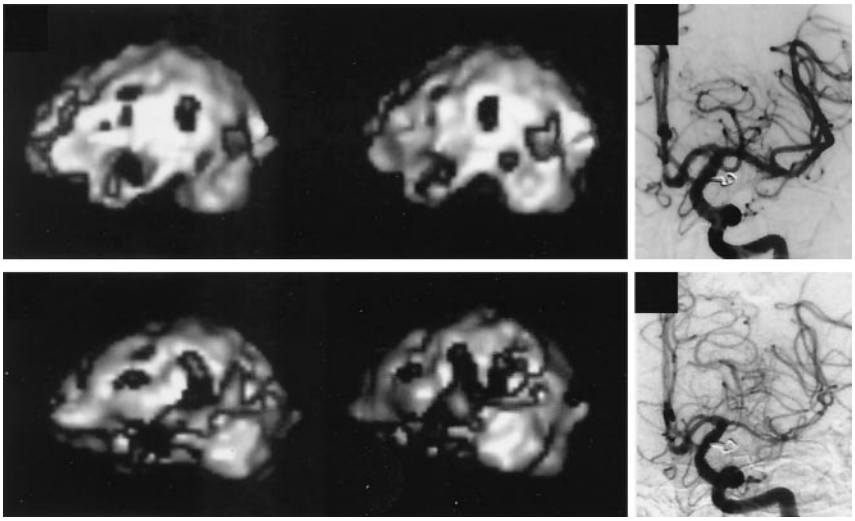

FIG 4. Serial changes in cortical rCBF in a case with DIND.

Top left, Six days after the onset of SAH, 3D images show multiple, patchy areas of decreased cortical rCBF.

Top right, cerebral angiography performed on the same day reveals no angiographic vasospasm.

Bottom left, Ten days after the onset of SAH, 3D images show the widely decreased cortical rCBF.

Bottom right, Diffuse angiographic vasospasm is seen on an cerebral angiogram obtained on the same day.

luminal narrowing in the proximal main arteries that affected the rCBF. For example, transcranial Doppler (TCD) sonography is often used for the early detection of cerebral vasospasm. Sometimes, however, TCD imaging cannot depict the increased flow velocity in the main arteries despite the occurrence of ischemic symptoms due to cerebral vasospasm (25). This false-negative TCD finding has been attributed to vasospasm of peripheral sites (26). Therefore, this would confirm that a peripheral type of angiographic vasospasm or microcirculatory disturbance is not unlikely to affect CBF during cerebral vasospasm (19, 26).

That is why the peripheral portion of those arteries was also analyzed in relation to the rCBF, in addition to proximal main arteries, in this study. In the evaluation of the rCBF in the ROI on 2D images, the differences of CBF changes among each type of angiographic vasospasm were not statistically significant. Therefore, the degree of rCBF decrease in the ischemic core does not differ according to the type of angiographic vasospasm. The global region, which was evaluated for the mean hemispheric CBF in this study, was mostly affected by the combined type of angiographic vasospasm, which resulted in a decreased mean hemispheric CBF. In addition, no statistically significant differences were seen between the types of angiographic vasospasm. Analysis of 3D images revealed that the CBF in the cerebral cortex was particularly affected by the type of angiographic vasospasm. This was especially true with peripheral arterial spasm regardless of the presence of proximal arterial spasm, which is well correlated to decreased cortical rCBF shown on 3D images. Therefore, when TCD imaging fails to indicate a luminal narrowing of the main arteries, an evaluation of the decreased cortical rCBF may be useful in estimating the presence of the peripheral type of angiographic vasospasm. In combination with either CT angiography (27) or MR angiography (28), this would obviate cerebral angiography.

In our cases with DIND, the rCBF in the ROI shown on 2D images was significantly reduced, and the area of decreased cortical rCBF shown on 3D images was significantly increased. However, the mean hemispheric CBF was not significantly different between the cases with DIND and those without DIND. This finding indicates that the decreased rCBF that caused the DIND does not always affect the global or hemispheric CBF (7). In previous studies, the relationships of CBF to size of the infarction due to cerebral vasospasm and the patients' prognosis were not fully investigated (8, 18). This study did show that the extent of decreased cortical rCBF on 3D SPECT images was well correlated with both the size of infarction and the patients' prognosis. Therefore, evaluating the extent of the decreased cortical CBF shown on 3D images can provide useful information for predicting a patient's prognosis.

In this study, a cortical region with flow less than 30 mL/100 g/min was displayed as an image defect on the 3D display. This category included various ischemic states, such as a CBF under the electrical failure threshold or a CBF under the membrane failure threshold (29). A CBF between these two thresholds was considered to be an ischemic penumbra, and it was thought to be reversible (29, 30). Until now, this reversibility was believed to depend solely on the duration of the decreased rCBF (31). The results of this study suggest that this reversibility is also affected by the extent of the lesion. Our finding is supported by those of other recent studies of ischemic penumbra (31). These studies indicate that the ischemic penumbra is not just a topographic locus but also a dynamic (time $\times$ space) process and that it is characterized by an evolving zone of bioenergetic upheaval (31, 32).

The prompt institution of appropriate therapy to decrease vasospasm depends on the ability to predict impending vasospasm or to diagnose vasospasm early. Although TCD sonography has been the standard diagnostic method for this purpose, it is limited in its diagnostic accuracy (25, 26). In this report, we have documented patchy cortical image defects that occurred before the onset of DIND in those cases in which DIND developed. The etiology of these patchy defects is unclear. Factors other than angiographic vasospasm may be the cause, because angiographic

vasospasm was not marked at this stage. PET studies have indicated that the cerebral metabolic rate of oxygen decreases in the acute stage of SAH (14, 15, 17, 37). In particular, some studies have shown that the reduction in the cerebral metabolic rate of oxygen is accompanied by a decreased CBF that is not related to cerebral vasospasm in the acute stage of SAH (17, 33). In fact, this may be the cause of the patchy cortical decreased rCBF that leads to cerebral vasospasm vulnerability later on. Further studies are needed to confirm this hypothesis. Because SPECT study is less invasive than other studies, the finding of patchy, decreased cortical rCBF on SPECT images might be useful in predicting cerebral vasospasm. When patchy, decreased cortical rCBF is identified, radically induced hypertension and hypervolemic therapy can be started, or prophylactic intraarterial papaverine infusion and balloon angioplasty can be considered, even before the onset of DIND.

Conclusion

The finding of decreased cortical rCBF on the 3D images was shown to be significantly more likely in cases with DIND, in cases with a large infarction due to vasospasm, and in cases with a poor prognosis after vasospasm. These increases were also related to the type of angiographic vasospasm; the greatest decrease in cortical rCBF occurred in the combined type (a combination of the peripheral and proximal types) of vasospasm, and it was followed, in order, by the peripheral type, the proximal type, and the cases with no angiographic vasospasm. Of note, in the cases with DIND, patchy areas of decreased cortical rCBF were seen before the onset of DIND. An analysis of the type and extent of decreased cortical rCBF shown on the 3D SPECT images is useful in evaluating a patient's clinical condition during vasospasm, in predicting the patient's prognosis, and in predicting the occurrence of vasospasm.

References

1. Fukui MB, Johnson DW, Yonas H, Sekhar L, Latchaw RE, Pentheny S. **Xe/CT cerebral blood flow evaluation of delayed symptomatic cerebral ischemia after subarachnoid hemorrhage.** *AJNR Am J Neuroradiol* 1992;13:265–270
2. Jakobsen M, Overgaard J, Marcussen E, Enevoldsen EM. **Relation between angiographic cerebral vasospasm and regional CBF in patients with SAH.** *Acta Neurol Scand* 1990;82:109–115
3. Mickey B, Vorstrup S, Voldby B, Lindewald H, Harmsen A, Lassen NA. **Serial measurement of regional cerebral blood flow in patients with SAH using 133Xe inhalation and emission computerized tomography.** *J Neurosurg* 1984;60:916–922
4. Powsner RA, O'Tuama LA, Jabre A, Melhem ER. **SPECT imaging in cerebral vasospasm following subarachnoid hemorrhage.** *J Nucl Med* 1998;39:765–769
5. Hatazawa J, Iida H, Shimosegawa E, Sato T, Murakami M, Miura Y. **Regional cerebral blood flow measurement with iodine-123-IMP autoradiography: normal values, reproducibility and sensitivity to hypoperfusion.** *J Nucl Med* 1997;38:1102–1108
6. Voldby B, Enevoldsen EM, Jensen FT. **Regional CBF, intraventricular pressure, and cerebral metabolism in patients with ruptured intracranial aneurysms.** *J Neurosurg* 1985;62:48–58
7. Heilbrun MP, Olesen J, Lassen NA. **Regional cerebral blood flow studies in subarachnoid hemorrhage.** *J Neurosurg* 1972;37:36–44
8. Ishii R. **Regional cerebral blood flow in patients with ruptured intracranial aneurysms.** *J Neurosurg* 1979;50:587–594
9. Granowska M, Britton KE, Afshar F, Wright CW, Smyth RR, Lee TY, Nimmon CC. **Global and regional cerebral blood flow. Noninvasive quantitation in patients with subarachnoid hemorrhage.** *J Neurosurg* 1980;53:153–159
10. Kelly PJ, Gorten RJ, Grossman RG, Eisenberg HM. **Cerebral perfusion, vascular spasm, and outcome in patients with ruptured intracranial aneurysms.** *J Neurosurg* 1977;47:44–49
11. Geraud G, Tremoulet M, Guell A, Bes A. **The prognostic value of noninvasive CBF measurement in subarachnoid hemorrhage.** *Stroke* 1984;15:301–305
12. Naderi S, Ozguven MA, Bayhan H, Gokalp H, Erdogan A, Egemen N. **Evaluation of cerebral vasospasm in patients with subarachnoid hemorrhage using single photon emission computed tomography.** *Neurosurg Rev* 1994;17:261–265
13. Hasan D, van Peski J, Loeve I, Krenning EP, Vermeulen M. **Single photon emission computed tomography in patients with acute hydrocephalus or with cerebral ischaemia after subarachnoid haemorrhage.** *J Neurol Neurosurg Psychiatry* 1991;54:490–493
14. Kawamura S, Sayama I, Yasui N, Uemura K. **Sequential changes in cerebral blood flow and metabolism in patients with subarachnoid haemorrhage.** *Acta Neurochir (Wien)* 1992;114:12–15
15. Hino A, Mizukawa N, Tenjin H, Imahori Y, Taketomo S, Yano I, Nakahashi H, Hirakawa K. **Postoperative hemodynamic and metabolic changes in patients with subarachnoid hemorrhage.** *Stroke* 1989;20:1504–1510
16. Powers WJ, Grubb RL Jr., Baker RP, Mintun MA, Raichle ME. **Regional cerebral blood flow and metabolism in reversible ischemia due to vasospasm: determination by positron emission tomography.** *J Neurosurg* 1985;62:539–546
17. Grubb RL Jr., Raichle ME, Eichling JO, Gado MH. **Effects of subarachnoid hemorrhage on cerebral blood volume, blood flow, and oxygen utilization in humans.** *J Neurosurg* 1977;46:446–453
18. Davis S, Andrews J, Lichtenstein M, et al. **A single-photon emission computed tomography study of hypoperfusion after subarachnoid hemorrhage.** *Stroke* 1990;21:252–259
19. Ohkuma H, Manabe H, Tanaka M, Suzuki S. **Impact of cerebral microcirculatory changes on cerebral blood flow during cerebral vasospasm after aneurysmal subarachnoid hemorrhage.** *Stroke* 2000;31:1621–1627
20. Wallis JW, Miller TR. **Three-dimensional display in nuclear medicine and radiology.** *J Nucl Med* 1991;32:534–546
21. Wallis JW, Miller TR. **Volume rendering in three-dimensional display of SPECT images.** *J Nucl Med* 1990;31:1421–1430
22. Iida H, Itoh H, Nakazawa M, et al. **Quantitative mapping of regional cerebral blood flow using iodine-123-IMP and SPECT.** *J Nucl Med* 1994;35:2019–2030
23. Ito H, Ishii K, Atsumi H, et al. **Error analysis of table look-up method for cerebral blood flow measurement by 123I-IMP brain SPECT: comparison with conventional microsphere model method.** *Ann Nucl Med* 1995;9:75–80
24. Iida H, Akutsu T, Endo K, et al. **A multicenter validation of regional cerebral blood flow quantitation using [123I]iodoamphetamine and single photon emission computed tomography.** *J Cereb Blood Flow Metab* 1996;16:781–793
25. Lysakowski C, Walder B, Costanza MC, Tramer MR. **Transcranial Doppler versus angiography in patients with vasospasm due to a ruptured cerebral aneurysm: a systematic review.** *Stroke* 2001;32:2292–2298
26. Okada Y, Shima T, Nishida M, Yamane K, Hatayama T, Yamanaka C, Yoshida A. **Comparison of transcranial Doppler investigation of aneurysmal vasospasm with digital subtraction angiographic and clinical findings.** *Neurosurgery* 1999;45:443–450
27. Anderson GB, Ashforth R, Steinke DE, Findlay JM. **CT angiography for the detection of cerebral vasospasm in patients with acute subarachnoid hemorrhage.** *AJNR Am J Neuroradiol* 2000;21:1011–1015
28. Grandin CB, Cosnard G, Hammer F, Duprez TP, Stroobandt G, Mathurin P. **Vasospasm after subarachnoid hemorrhage: diagnosis with MR angiography.** *AJNR Am J Neuroradiol* 2000;21:1611–1617
29. Siesjo BK. **Pathophysiology and treatment of focal cerebral ischemia. Part I: Pathophysiology.** *J Neurosurg* 1992;77:169–184
30. Heiss WD. **Experimental evidence of ischemic thresholds and functional recovery.** *Stroke* 1992;23:1668–1672
31. Baron JC. **Mapping the ischaemic penumbra with PET: a new approach.** *Brain* 2001;124(pt 1):24
32. Hakim AM. **Ischemic penumbra: the therapeutic window.** *Neurology* 1998;51(3 suppl 3):S44–S46
33. Hayashi T, Suzuki A, Hatazawa J, et al. **Cerebral circulation and metabolism in the acute stage of subarachnoid hemorrhage.** *J Neurosurg* 2000;93:1014–1018